Quantum Interference Effects in the Vibrational Relaxation of the O–H Stretch Overtone of Liquid H_2O

Sietse T. van der Post[1], Sander Woutersen[2], Huib J. Bakker[1,2]

[1] *FOM Institute AMOLF, Science Park 104, Amsterdam, The Netherlands*

[2] *Van 't Hoff Institute for Molecular Sciences, University of Amsterdam, Science Park 904, Amsterdam, The Netherlands**

(Dated: April 7, 2016)

Abstract

We study the vibrational relaxation of the O–H stretch vibrations of liquid H_2O after excitation of the overtone transition with femtosecond two-color infrared pump-probe spectroscopy. The overtone transition has its maximum at 6900 cm^{-1} (1.45 μm), which is a relatively high frequency in view of the central frequency of 3400 cm^{-1} of the fundamental transition. The excitation of the overtone leads to a transient induced absorption of two-exciton states of the O–H stretch vibrations. When the overtone excitation frequency is tuned from 6600 to 7200 cm^{-1}, the vibrational relaxation time constant of the two-exciton states increases from 400±50 fs to 540±40 fs. These values define a limited range of relatively long relaxation time constants compared to the range of relaxation time constants of 250-550 fs that we recently observed for the one-exciton O–H stretch vibrational state of liquid H_2O (S.T. van der Post et al., *Nature Comm.* **2015**, *6*, 8384). We explain the high central frequency and the limited range of relatively long relaxation time constants of the overtone transition from the destructive quantum interference of the mechanical and electrical anharmonic contributions to the overtone transition probability. As a result of this destructive interference, the overtone transition of liquid H_2O is dominated by molecules of which the O–H groups donate relatively weak hydrogen bonds to other H_2O molecules.

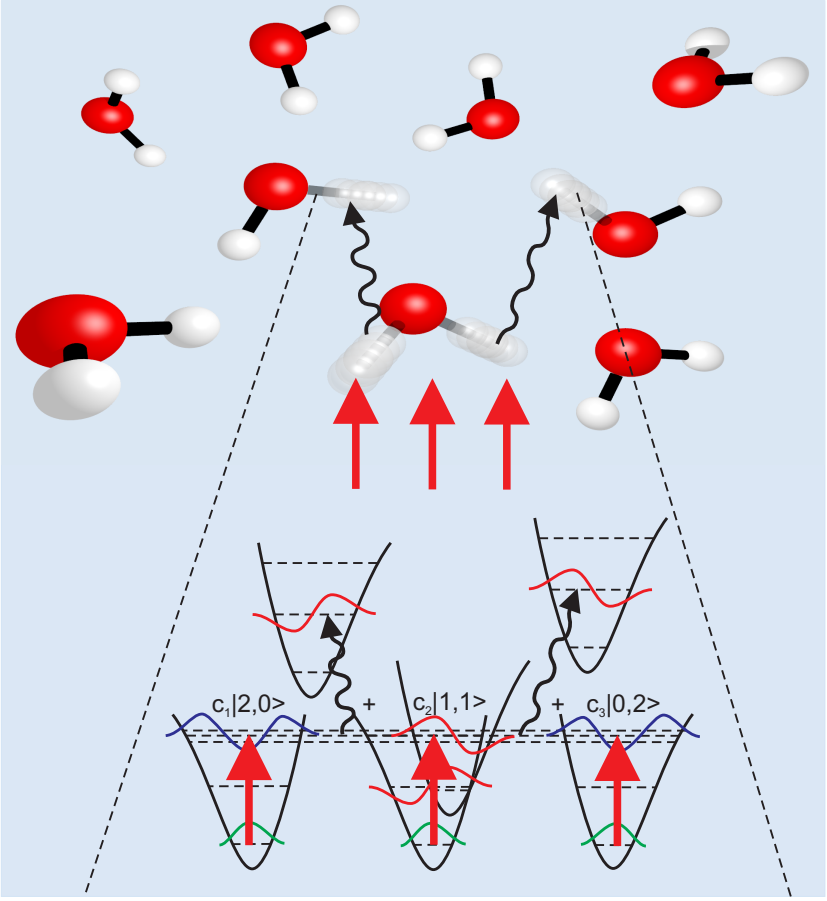

Introduction

The linear infrared absorption and Raman spectra of the fundamental O–H stretch vibrations of liquid water are complex bands that show distinct structure[1,2]. This structure is largely the result of the strong resonant intra- and intermolecular couplings of the O–H stretch vibrations of the H_2O molecules[1–11]. The intramolecular coupling leads to the formation of symmetric and asymmetric vibrations, and the intermolecular coupling leads to the formation of excitonic O–H stretch vibrational states that are delocalized over several H_2O molecules[5,6,9–14]. In addition, the symmetric O–H stretch vibration shows a Fermi resonance with the overtone of the H_2O-bend vibration thereby complicating the spectrum even further[5,6,15–17].

The structure of the linear absorption and Raman spectra vanishes in case water is isotopically diluted. In the case of a dilute solution of HDO molecules in D_2O, the O–H stretch vibration is spectrally well separated from the O–D vibrations, thus switching off the effects of resonant intra- and intermolecular coupling on the spectrum of the O–H stretch vibration. In addition, for HDO the O–H stretch vibration is no longer in resonance with the overtone of the bending mode. As a

result, the linear absorption and Raman spectra of the O–H stretch vibration of HDO dissolved in D_2O have a near-gaussian shape.

The overtone spectra of molecular vibrations usually show a more complex structure than the spectra of the fundamental transitions. For instance, the overtone spectrum of the O–H stretch vibration of HDO dissolved in D_2O contains several closely-spaced peaks[18]. These peaks have been explained from the presence of different hydrogen-bonding species in water[1,19–21]. However, Sceats et al. explained the structure of the O–H stretch overtone spectrum of HDO:D_2O from the quantum interference of different anharmonic contributions to the transition probability of the overtone transition[18]. The overtone transition is forbidden in a harmonic approximation, meaning that a non-zero cross-section for this transition relies on the presence of electrical and mechanical anharmonicities. Sceats et al. showed that these anharmonicities cancel each other for HDO molecules showing particular hydrogen-bond strengths, thus providing distinct structure to the O–H stretch overtone spectrum of HDO:D_2O[18].

In view of the structured shape of the fundamental spectrum of liquid H_2O and that of the overtone spectrum of HDO:D_2O, it is quite surprising that the O–H stretch overtone spectrum of H_2O has the form of a relatively narrow, smooth single band[22,23]. In this paper we investigate the origin of the spectral shape of the overtone of the O–H stretch vibration of liquid H_2O, and we study the vibrational relaxation dynamics following excitation of this transition.

Experiment

We measure the vibrational relaxation dynamics of the overtone transition of liquid H_2O with femtosecond two-color pump-probe spectroscopy. We use an intense near-infrared laser pulse (the pump) to excite the O–H stretch overtone of a small fraction of the H_2O molecules. This excitation leads to transient absorption changes that are monitored with a weak, independently tunable infrared probe pulse that is delayed with respect to the pump pulse. We determine the relaxation of the vibrational excitation by measuring the absorption changes as a function of the delay time between the probe and the pump pulse.

The near-infrared pump pulses are generated via optical parametric amplification in a β-bariumborate (BBO) crystal (Light-Conversion TOPAS). This process is pumped with 1 mJ, 35 femtosecond, 800 nm pulses (repetition rate 1 kHz) delivered by an amplified Ti:sapphire laser system (Coherent Legend Elite). The parametric amplification leads to the generation of signal

and idler pulses in the frequency range of 4000–8500 cm^{-1} (2500–1200 nm). The overtone transition of the O–H stretch vibrations is excited with signal pulses with a central frequency that is tuned between 6600 and 7200 cm^{-1}. The spectral bandwidth of the pulses is 250 cm^{-1} (FWHM), the pulse duration is $\sim$100 femtoseconds, and the pulse energy is $\sim$90 μJ.

We use a relatively thick water sample with a path length of 100 μm to obtain sufficient optical density at the overtone transition to perform the two-color pump-probe experiment. For this sample, the optical density at the frequency of 3400 cm^{-1} of the fundamental ($v = 0 \rightarrow 1$) transition of the O–H stretch vibration is $>$30, making it impossible to probe the fundamental transition. The sample is sufficiently transparent at frequencies $<$3000 cm^{-1} to probe the absorption changes induced by the excitation of the overtone transition in this frequency region.

The mid-infrared probe pulses are produced as follows. We generate signal and idler pulses with a home-built optical parametric amplifier (OPA) that is pumped with 0.5 mJ, 35 femtosecond, 800 nm pulses delivered by the same amplified Ti:sapphire laser system (Coherent Legend Elite) that is used to generate the pump pulse. The signal pulses can be tuned in the frequency range 6250–9000 cm^{-1} (1100-1600 nm), and the idler pulses in the frequency range 3500–6250 cm^{-1} (1600-2700 nm). The signal and idler pulses are sent into a silver-gallium-disulfide crystal to generate pulses at their difference frequency. The resulting mid-infrared pulses are broadly tunable and have a spectral bandwidth of $\sim$250 cm^{-1} (FWHM), a pulse duration of $\sim$100 femtoseconds, and a pulse energy of $\sim$400 nJ. The pulses are split into two parts. One of these parts is used as a reference, the other part is sent into a delay line and is used as a probe to monitor the absorption changes induced by the pump pulse.

Pump, probe and reference pulses are focused into the water sample with a parabolic mirror, but only the pump and the probe are in spatial overlap. The pump beam is chopped at 500 Hz, meaning that every other pump pulse is blocked. We use this procedure to optimize the signal-to-noise ratio of the pump-induced signal. After the sample the probe and reference pulses are sent into a spectrograph and dispersed on two lines of a 3x32 pixel mercury-cadmium-telluride infrared detector array (Infrared Associates). The dispersed reference signal is used to obtain a frequency-resolved shot-to-shot normalization of the probe pulse energy. The pump energy is quite high and potentially could lead to the production of electrons in the sample via multi-photon ionization processes. These photo-generated electrons would give rise to an induced absorption signal that depends in a highly non-linear manner on the pump energy. Therefore, in all experiments we checked whether the signal rises linearly with the pump-pulse energy, to ensure that the measured

signal does not contain any contribution from photo-generated electrons.

The water sample cannot be contained in between two infrared-transparent windows, as the high photon and pulse energy of the pump pulses would lead to white-light generation in these windows. Therefore, the experiments are performed with a wire-flow cell[24] that is constructed as follows. Water from a reservoir is gently released from a flat nozzle bearing an elongated tungsten wire loop of 125 μm thickness. The width of the loop is approximately 5 mm. At the bottom of the tungsten wire loop the water is collected in a glass funnel and pumped back into the reservoir using a peristaltic pump. Due to the high surface tension of water, a stable thin film is formed in between the wires. The thickness of the water film depends on the flow rate and vertical distance from the nozzle. The flow rate is increased by increasing the elevation difference between the nozzle and the water level in the reservoir. The film becomes thinner for lower flow rates and at positions further away from the nozzle due to the gravitational pull on the water. Stable configurations were obtained with film thicknesses of 25–125 μm.

Results

Fig. 1 shows the linear absorption spectrum of liquid H_2O. A linear spectrum taken from the film close to the nozzle using a fast flow rate closely resembles a linear spectrum from a water-filled conventional sample cell with 115 μm optical path length. For this optical path length the absorbance of a pure H_2O sample is $\sim$0.2 OD at the maximum of the absorption band of the overtone of the O–H stretch vibrations.

Fig. 2a shows transient spectra in the frequency region below 3000 cm^{-1} following excitation of the overtone transition of the O–H stretch vibration of liquid H_2O at 7000 cm^{-1}. The transient spectrum shows an induced absorption centered at 2850 cm^{-1}. The induced absorption signal cannot be the result of the transient excitation of low-frequency hydrogen bonds, as such an excitation would lead to a bleaching and blue-shift of the fundamental $v = 0 \rightarrow 1$ absorption spectrum of water (centered at 3300 cm^{-1}), and thus to a bleaching signal instead of an induced absorption signal at frequencies $<$3000 cm^{-1}. Instead, the induced absorption is likely associated with the excited $v = 1$ and/or $v = 2$ states of the O–H stretch vibrations. The induced absorption signal rises instantaneously (following the pump-probe cross-correlation), and decays on a time scale of $\sim$500 femtoseconds. In Fig. 2b the transient absorption signal measured at 2750 cm^{-1} is shown as a function of the time delay with respect to the excitation pulse. The signal is shown for four

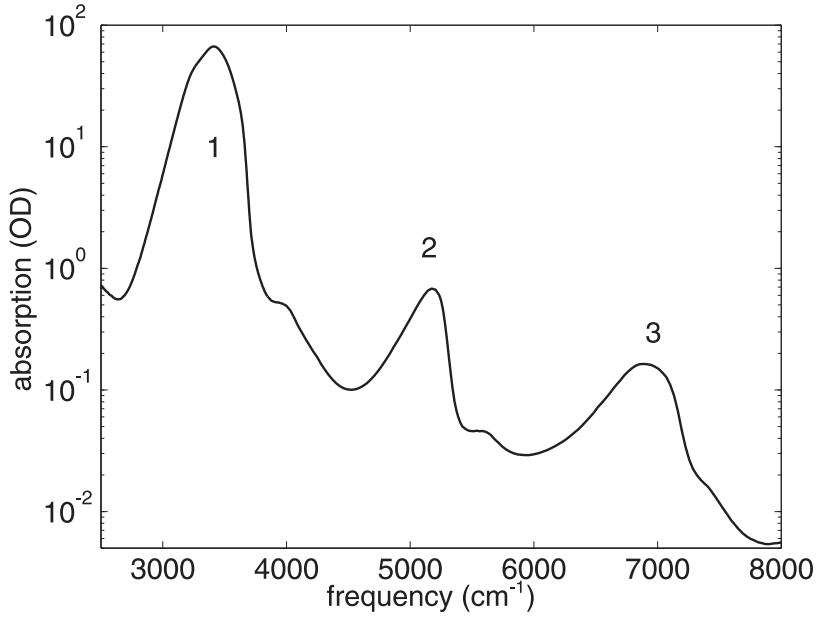

FIG. 1: Logarithmic plot of the linear spectrum of liquid H_2O (scaled to an equivalent path length of 115 μm) and the water film used in the experiment. The spectrum shows the fundamental O–H stretch absorption band (1) centered at 3400 cm^{-1} (1), the OH-stretch/H_2O-bend combination band centered at 5150 cm^{-1} (2), and the overtone of the O–H stretch vibrations centered at 6900 cm^{-1} (3).

different excitation pulses with central frequencies of 6600, 6800, 7000, and 7200 cm^{-1}. The signals near delay zero shows a somewhat erratic character that can be assigned to a coherent artifact resulting from the high energy of the excitation pulse. For delays >300 fs, the signals show an exponential decay. The decay of the signal becomes slower with increasing central frequency of the excitation pulse.

Fig. 2a shows that the transient absorption signal relaxes to a bleaching signal. This bleaching signal can be explained from a heating effect. The energy of the vibrational excitation is eventually equilibrated over all degrees of freedom in the focus of the excitation pulses, which corresponds to an increase of the sample temperature. Since the linear absorption spectrum changes with temperature, the thermalization of the excitation energy leads to a non-zero thermal difference spectrum. At intermediate delay times, the transient absorption spectra represent a combination of the excited state response and the thermal difference spectrum. To determine the vibrational relaxation time T_1, we disentangle these contributions by fitting a kinetic model to the data. In this model the excited state decays with time constant T_1 to an intermediate state that subsequently

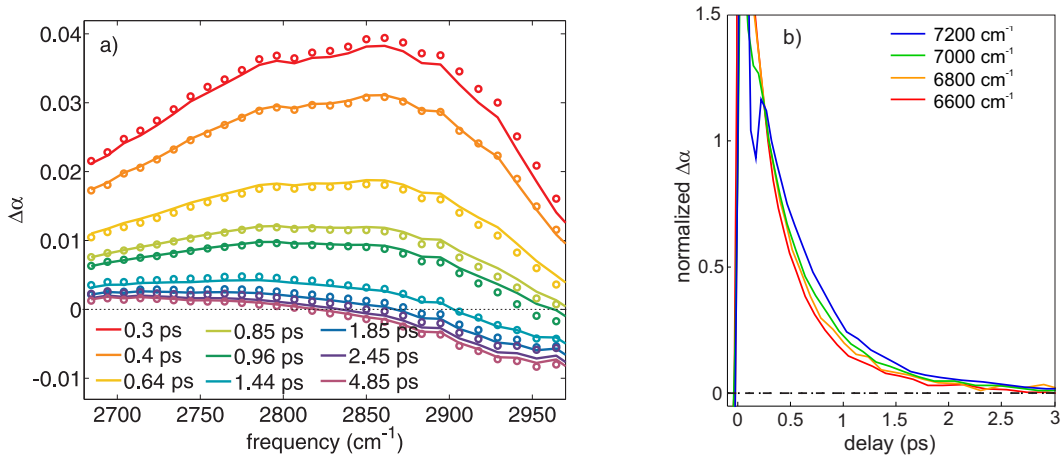

FIG. 2: (**a**) Transient spectra obtained from a measurement in which the OH-stretch overtone was pumped at 7000 cm^{-1} and the frequency region <3000 cm^{-1} was probed. The transient spectra show an induced absorption centered at 2850 cm^{-1}. The solid lines result from the modeling of the data with a kinetic spectral decomposition model[25] (**b**) Transient absorption signal $\Delta\alpha$ at 2750 cm^{-1} following excitation of the overtone transition of the O–H stretch as a function of delay with respect to the excitation pulse. The transient absorption signal is shown for four excitation pulses with different central frequencies, as indicated in the inset. To facilitate the comparison of the relaxation dynamics the transient absorption signals are normalized to the signal measured at a delay time of 300 fs.

decays with a time constant τ_{eq} to a final thermalized state. This kinetic model has been used before to describe the relaxation of the O–D stretch vibration of HDO molecules dissolved in H_2O[25]. The solid lines in Fig. 2a represent the results of the fit.

In Fig. 3 the value of the relaxation time constant T_1 is shown as a function of the frequency of the pump pulse used to excite the overtone transition. The T_1 values vary between 400±50 fs and 540±40 fs. These values are much longer than the T_1 relaxation time constants of 200-260 fs that have been reported in earlier femtosecond mid-infrared studies of the vibrational relaxation following excitation of the fundamental $v = 0 \rightarrow 1$ transition of the O–H stretch vibrations of liquid H_2O[3–6,9,10,26,27]. Recently, we measured the frequency dependence of the T_1 time constant of the fundamental transition, and we found that this time constant varies from 250-550 fs when the excitation frequency is tuned from 3100 to 3700 cm^{-1}.[11] Clearly, the range of time constants of 400 - 540 fs observed for the overtone is much smaller than the range of time constants observed for the fundamental transition of H_2O.

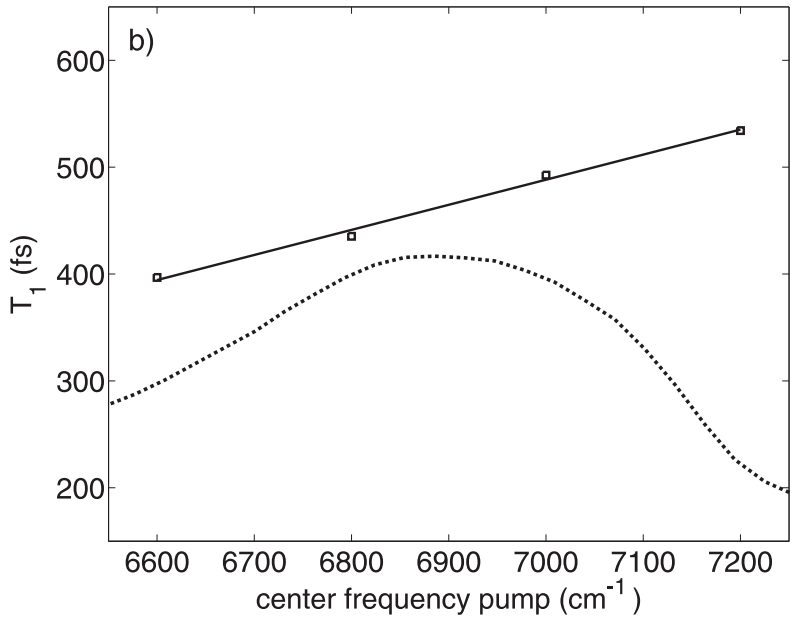

FIG. 3: The vibrational relaxation times T_1 of the $v = 2$ state after excitation of the OH-stretch overtone at different frequencies (horizontal axis). Excitation of the blue shoulder of the overtone leads to a longer T_1 compared to an excitation at the red shoulder. The dotted line is the shape of the linear spectrum of the overtone band.

Theory

In liquid H_2O, the local O–H vibrations are strongly interacting leading to the formation of delocalized exciton states. These exciton states exist both on the single vibrational quantum level and on the double vibrational quantum level.

Following the treatment of Ref.[28] we write the Hamiltonian of the system as:

$$H = \sum_{i,a} \epsilon_{ia} b_{ia}^{\dagger} b_{ia} + \sum_{i,a<j,b} \beta_{ia,jb} (b_{ia}^{\dagger} b_{jb} + b_{jb}^{\dagger} b_{ia}), \tag{1}$$

with ϵ_{ia} the local O–H oscillator energies and $\beta_{ia,jb}$ the coupling between different O–H oscillators. The indices i and j refer to different H_2O molecules and the indices a and b refer to the two O–H vibrations located on the same H_2O molecule ($a, b = \{1, 2\}$). In this treatment we neglect the coupling to low-frequency modes (hydrogen bonds) that will lead to fluctuations (spectral diffusion) of the local O–H stretch vibrational energy levels.

The one-exciton states $|k\rangle$ can be created from the local states in the following way:

$$|k\rangle = \sum_{i,a} q_{kia} b_{ia}^{\dagger} |0\rangle_{ia}, \tag{2}$$

where $|0\rangle$ represents the direct-product state of local oscillators that are all in the ground state. The label ia implies that the creation operator $b_{ia}^{\dagger}$ acts on the local state of oscillator ia. The coefficients q_{kia} are obtained by diagonalizing the Hamiltonian of equation (1) considering only single local excitations. The coefficients q_{kia} are thus determined by the couplings $\beta_{ia,jb}$ between the different local states. The harmonic Hamiltonian of equation (1) conserves the number of excitations and can thus be separated in Hamiltonians describing the ground state, the one-exciton states, the two-exciton states, etc.

The two-exciton states $|kl\rangle$ can be created by subsequent application of two creation operators:

$$|kl\rangle = \sum_{i,a,j,b} a_{kl} q_{ljb} b_{jb}^{\dagger} q_{kia} b_{ia}^{\dagger} |0\rangle_{ia,jb} \tag{3}$$

where the normalization factor a_{kl} =1 in case $k \neq l$ and a_{kl} =1/$\sqrt{2}$ in case $k = l$. The state $|0\rangle_{ia,jb}$ is again a product state of local oscillators that are all in the vibrational ground state, with the label ia, jb indicating that the creation operators subsequently act on local oscillators ia and jb, which can be the same (corresponding to an excitation of a local $v = 2$ state). The delocalized two-exciton states are thus mixtures of local $v = 2$ vibrational states and double excitations of $v = 1$ states of local O–H oscillators.

The transition dipole moment associated with the overtone transition to the two-exciton state $|kl\rangle$ can be written as:

$$\langle kl|\hat{\mu}|0\rangle = a_{kl} \left\{ \sum_{i,a} \sqrt{2} q_{kia} q_{lia} \langle 2|\hat{\mu}|0\rangle_{ia} + \sum_{i,a,j,b} q_{ljb} q_{kia} \langle 1,1|\hat{\mu}|0,0\rangle_{ia,jb} \right\}, \tag{4}$$

where the bras and kets on the left-hand side refer to exciton state and the bras and kets on the right-hand side refer to local O–H stretch vibrations. The dipole moment operator $\hat{\mu}$ reflects the distribution of charges q_i in a molecule and can be expanded in the local mode coordinates:

$$\hat{\mu} = \sum_{i,a} \frac{d\hat{\mu}}{dr_{ia}} r_{ia} + \sum_{i,a} \frac{1}{2} \frac{d^2\hat{\mu}}{dr_{ia}^2} r_{ia}^2 + \sum_{i} \frac{d^2\hat{\mu}}{dr_{i1} dr_{i2}} r_{i1} r_{i2} + \cdots \tag{5}$$

The last two terms of this expression represent a nonlinear dependence of the dipole moment on the local vibrational coordinates. By explicitly accounting for these two terms we assume that the derivative of the dipole with respect to local coordinate r_{i1} will only show a significant dependence on the local vibrational coordinates in the same molecule, i.e. r_{i1} and r_{i2}. Substitution

of expression (5) for $\hat{\mu}$ in equation(4) yields:

$$\langle kl|\hat{\mu}|0\rangle = a_{kl}\sum_i\left\{\sum_a\sqrt{2}q_{kia}q_{lia}\left[\frac{d\hat{\mu}}{dr_{ia}}\langle 2|r_{ia}|0\rangle+\frac{1}{2}\frac{d^2\hat{\mu}}{dr_{ia}^2}\langle 2|r_{ia}^2|0\rangle\right]+ (q_{ki1}q_{li2}+q_{ki2}q_{li1})\frac{d^2\hat{\mu}}{dr_{i1}dr_{i2}}\langle 1|r_{i1}|0\rangle\langle 1|r_{i2}|0\rangle\right\} \quad (6)$$

The transition dipole moment to a delocalized two-exciton state containing two O–H vibrational excitations can thus be expressed as a sum of products of dipole-moment derivatives and matrix elements in local O–H stretch vibrational coordinates and wavefunctions. The two terms in the square brackets involve the excitation of a local O–H stretch vibration to its $v = 2$ state, and the last term corresponds to the simultaneous $v = 0 \rightarrow 1$ excitation of two O–H stretch vibrations located on the same H_2O molecule. The first term in the square brackets is only non-zero if the local vibrational states possess anharmonic character. This diagonal anharmonicity was not included in the Hamiltonian of equation (1) and can lead to mixing and energy shifts of the two-exciton states $|kl\rangle$. The second term in the square brackets and the last term are non-zero in case the dipole moment shows a nonlinear dependence on the local vibrational coordinates.

The character of the different local $v_{ia} = 1$ and $v_{ia} = 2$ states that enter the matrix elements $\langle 1|r_{ia}|0\rangle$, $\langle 2|r_{ia}|0\rangle$, $\langle 2|r_{ia}^2|0\rangle$ of equation (6) depend on the strength of the local hydrogen-bond interactions, in particular on the strength of the hydrogen bond that is donated by the O–H group. In the following we will replace the different $v_{ia} = 1$ and $v_{ia} = 2$ states by single $v_{OH} = 1$ and $v_{OH} = 2$ states. The character of these single $v_{OH} = 1$ and $v_{OH} = 2$ states are an average of the local states contributing to the two-exciton states. The average character and thus the value of the matrix elements strongly depends on the strength of the average hydrogen-bond of the two-exciton states. The average hydrogen-bond strength also determines the frequency ω_{kl} of the two-exciton state. Hence, the local matrix elements can be characterized by the corresponding two-exciton transition frequency ω_{kl}:

$$\langle kl|\hat{\mu}|0\rangle = a_{kl}\sum_i\left\{\sum_a\sqrt{2}q_{kia}q_{lia}\left[\frac{d\hat{\mu}}{dr_{OH}}\langle 2|r_{OH}|0\rangle(\omega_{kl})+\frac{1}{2}\frac{d^2\hat{\mu}}{dr_{OH}^2}\langle 2|r_{OH}^2|0\rangle(\omega_{kl})\right]+ (q_{ki1}q_{li2}+q_{ki2}q_{li1})\frac{d^2\hat{\mu}}{dr_{OH1}dr_{OH2}}\langle 1|r_{OH1}|0\rangle\langle 1|r_{OH2}|0\rangle(\omega_{kl})\right\} \quad (7)$$

The matrix elements in this expression represent average matrix elements and thus no longer depend on the local oscillator indices i and a. Therefore, we can replace $a_{kl}\sum_i\sum_a\sqrt{2}q_{kia}q_{lia}$ by δ_{kl}. We further assume that $\sum_i(q_{ki1}q_{li2}+q_{ki2}q_{li1}) = f_{kk}\delta_{kl}$, which implies that we assume that

the contributions of the different products $q_{ki1}q_{li2}$ cancel in case $k \neq l$, i.e. when the two-exciton state comprises two different (orthogonal) single-exciton states. We also note that $\sum_i (q_{ki1}q_{ki2} + q_{ki2}q_{ki1}) = 1$ in case $q_{ki1} = q_{ki2}$, i.e. when the two OH groups located on the same H_2O molecule contribute with equal amplitude and phase to the exciton state $|k\rangle$. Hence, we obtain:

$$\begin{aligned} \langle kl|\hat{\mu}|0\rangle \;=\; \delta_{kl} \Bigg[& \frac{d\hat{\mu}}{dr_{OH}} \langle 2|r_{OH}|0\rangle(\omega_{kk}) + \frac{1}{2}\frac{d^2\hat{\mu}}{dr_{OH}^2} \langle 2|r_{OH}^2|0\rangle(\omega_{kk}) \\ & + f_{kk} \frac{d^2\hat{\mu}}{dr_{OH1}dr_{OH2}} \langle 1|r_{OH1}|0\rangle\langle 1|r_{OH2}|0\rangle(\omega_{kk}) \Bigg], \end{aligned} \tag{8}$$

with ω_{kk} the transition frequency to the two-exciton state $|kk\rangle$.

The frequency-integrated overtone cross-section σ_{ov} to all two-exciton states $|kl\rangle$ can be written as:

$$\int d\omega_{\mathrm{ov}} \sigma_{\mathrm{ov}}(\omega_{\mathrm{ov}}) = \sum_{k,l} \frac{\pi\omega_{kl}}{3\hbar c\varepsilon_0} |\langle kl|\hat{\mu}|0\rangle(\omega_{kl})|^2 \tag{9}$$

with ω_{ov} the overtone transition frequency. Substitution of equation (8) in equation (9) yields:

$$\begin{aligned} \int d\omega_{\mathrm{ov}} \sigma_{\mathrm{ov}}(\omega_{\mathrm{ov}}) \;=\; & \frac{\pi}{3\hbar c\varepsilon_0} \sum_k \omega_{kk} \Bigg| \Bigg[\frac{d\hat{\mu}}{dr_{OH}} \langle 2|r_{OH}|0\rangle(\omega_{kk}) + \frac{1}{2}\frac{d^2\hat{\mu}}{dr_{OH}^2} \langle 2|r_{OH}^2|0\rangle(\omega_{kk}) \Bigg] \\ & + f_{kk} \frac{d^2\hat{\mu}}{dr_{OH1}dr_{OH2}} \langle 1|r_{OH1}|0\rangle\langle 1|r_{OH2}|0\rangle(\omega_{kk}) \Bigg|^2 \end{aligned} \tag{10}$$

We define all two-exciton states $|kk\rangle$ with transition frequencies ω_{kk} within a frequency interval $d\omega_{\mathrm{ov}}$ around ω_{ov} as $N(\omega_{\mathrm{ov}})d\omega_{\mathrm{ov}}$. The summation over k over the two-exciton states $|kk\rangle$ can then be replaced by an integral over $d\omega_{\mathrm{ov}}$. For the integrand we obtain:

$$\begin{aligned} \sigma_{\mathrm{ov}}(\omega_{\mathrm{ov}}) \;=\; & \frac{\pi\omega_{\mathrm{ov}} N(\omega_{\mathrm{ov}})}{3\hbar c\varepsilon_0} \Bigg| [\frac{d\hat{\mu}}{dr_{OH}} \langle 2|r_{OH}|0\rangle(\omega_{\mathrm{ov}}) + \frac{1}{2}\frac{d^2\hat{\mu}}{dr_{OH}^2} \langle 2|r_{OH}^2|0\rangle(\omega_{\mathrm{ov}}) \\ & + f(\omega_{\mathrm{ov}}) \frac{d^2\hat{\mu}}{dr_{OH1}dr_{OH2}} \langle 1|r_{OH1}|0\rangle\langle 1|r_{OH2}|0\rangle(\omega_{\mathrm{ov}}) \Bigg|^2, \end{aligned} \tag{11}$$

where we also replaced f_{kk} by its continuum limit $f(\omega_{\mathrm{ov}})$.

It follows from equation (11) that the transition probability to the two-exciton states can be fully expressed in dipole moment derivatives and matrix elements in O–H vibrational coordinates that are located on the same H_2O molecule. This is a direct consequence of the fact that the excitation probability of the two-exciton states relies on the anharmonic character of the O–H vibrations and the nonlinear dependence of the dipole moment on the displacement. Both these properties are determined by higher-order terms in the *intra*molecular potential energy of the H_2O molecules. The fact that the transition probability relies on single-molecule dipole derivatives and matrix

elements does not mean that the two-exciton states themselves would be localized on a single H_2O molecule. In fact these states can be highly delocalized, including significant contributions from $v_i = 1, v_j = 1$ excitations that are located on different O–H oscillators. These delocalized $v_i = 1, v_j = 1$ excitations can even dominate the excited delocalized two-exciton states. The single-molecular character of the excitation probability implies that the optical excitation of a set of two-exciton states will set the relative phases of the excited states such that the initial probability of finding the two O–H stretch excitations on the same molecule is $\sim$1. The two O–H excitations are initially thus very strongly bunched. However, after the impulsive excitation the two O–H excitations will rapidly be transferred to different H_2O molecules and thus separate, as a result of the phase evolution (quantum interference) of the excited set of two-exciton states.

Lippincott-Schroeder model

The matrix elements entering the expression of the overtone cross-section of equation (11) can be evaluated using the Lippincott-Schroeder (LS) model, which has been shown to provide a good description of the coupling between the O–H stretch vibration and the hydrogen-bond. The LS-potential is based on empirical data that describes the energy levels of the OH stretch vibration and is given by[29],

$$\begin{aligned} V_{LS}(r_{OH}, R_{OO}) =& D_{Ia}\left(1 - e^{-n_{Ia}(r_{OH}-r_0)^2/2r_{OH}}\right) + \\ & D_{Ib}\left(1 - e^{-n_{Ib}(R_{OO}-r_{OH}-r_0)^2/2(R_{OO}-r_{OH})}\right) \end{aligned} \tag{12}$$

where r_{OH} is the oxygen-hydrogen distance and R_{OO} is the oxygen-oxygen distance between the hydrogen-bonding water molecules. $D_{Ia} = 38750\,\mathrm{cm}^{-1}$ is the binding energy of the OH covalent bond, $N_{Ia} = 9.8\,\text{Å}^{-1}$ is the parameter defining the OH stretch vibrational frequency and $r_0 = 0.97\,\text{Å}$ is the O–H bond length in the gas phase. D_{Ib} and n_{Ib} are obtained from a comparison of the model to empirical values[29]. The potential is shown in Fig. 4a for an oxygen-oxygen distance $R_{OO} = 3.1\,\text{Å}$, which corresponds to a very weak hydrogen-bond.

We calculate the wavefunctions in the high-frequency coordinate r_{OH} of the LS-potential for different hydrogen-bond lengths R_{OO} using a Numerov integration scheme. Fig. 4a shows the calculated wavefunctions of the first four energy levels for $R_{OO} = 3.1\,\text{Å}$. The transition energies that correspond to the $v = 0 \rightarrow 1$, $v = 1 \rightarrow 2$, $v = 2 \rightarrow 3$ and $v = 0 \rightarrow 2$ transitions are shown as a function of hydrogen-bond length in Fig. 4b. Within the LS model, every hydrogen-bond

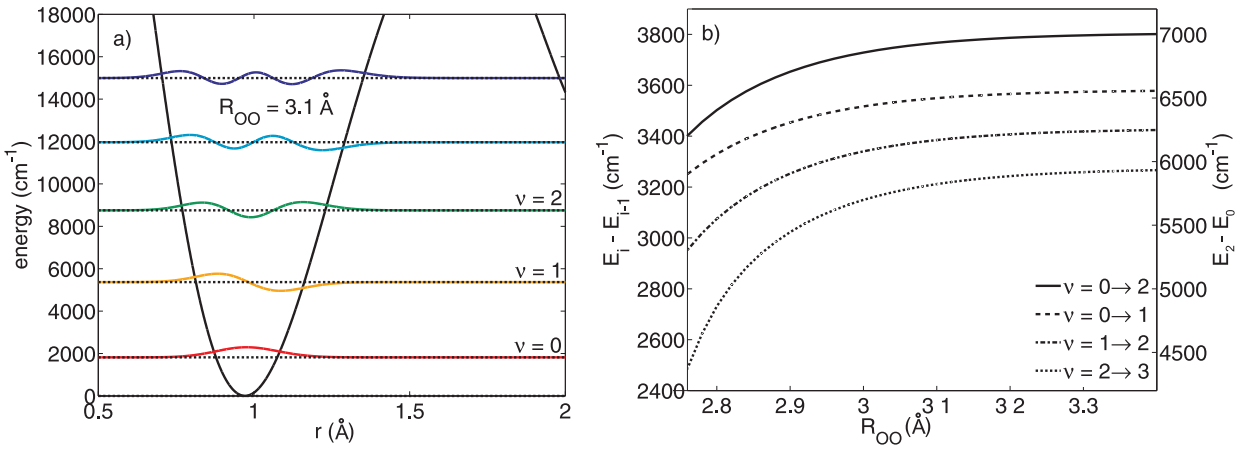

FIG. 4: a) The Lippincott-Schröder potential as a function of the O–H bond length r, for a hydrogen-bond length (oxygen-oxygen distance) of $R_{OO} = 3.1$ Å; b) The transition frequencies of $v = 0 \rightarrow 1$ (dashed), $v = 1 \rightarrow 2$ (dashed-dotted), $v = 2 \rightarrow 3$ (dashed-dotted), and $v = 0 \rightarrow 2$ (solid line, right axis) as a function of the hydrogen-bond lengths R_{OO}.

length R_{OO} leads to a discrete set of transition frequencies, because the O–H potential and thus the energy levels and wavefunctions of the high-frequency O–H coordinate only depend on the length R_{OO} of the hydrogen bond. This is an approximation as the transition frequency will also depend on the angle between the O–H coordinate and the O$\cdots$O coordinate. The distribution in angles will lead to a broadening of the O–H stretch absorption bands between the different levels. This broadening is relatively small compared to the width of the absorption bands resulting from the distribution in hydrogen-bond lengths[30–32].

Overtone absorption

We calculate the cross-section of the overtone transition $\sigma_{\mathrm{ov}}(\omega_{\mathrm{ov}})$ by evaluating the density, the dipole derivatives and the matrix elements that enter equations (11). The wave functions of the LS-potentials are used to evaluate the matrix elements $\langle 1|r_{OH}|0\rangle$, $\langle 2|r_{OH}|0\rangle$, $\langle 2|r_{OH}^2|0\rangle$ for a broad range of hydrogen-bond lengths. The results are shown in Fig. 5a.

The first derivative of the dipole moment $d\hat{\mu}/dr_{OH}$ was found to show the following empirical dependence on the fundamental transition frequency ω_{01}[18]:

$$\frac{d\hat{\mu}}{dr_{OH}}(\omega_{01}) \approx \left(-1.1934 + \sqrt{4.0448 + \frac{2.5966\omega_{01}}{\omega_f}}\right) \cdot 10^{-18} C. \qquad (13)$$

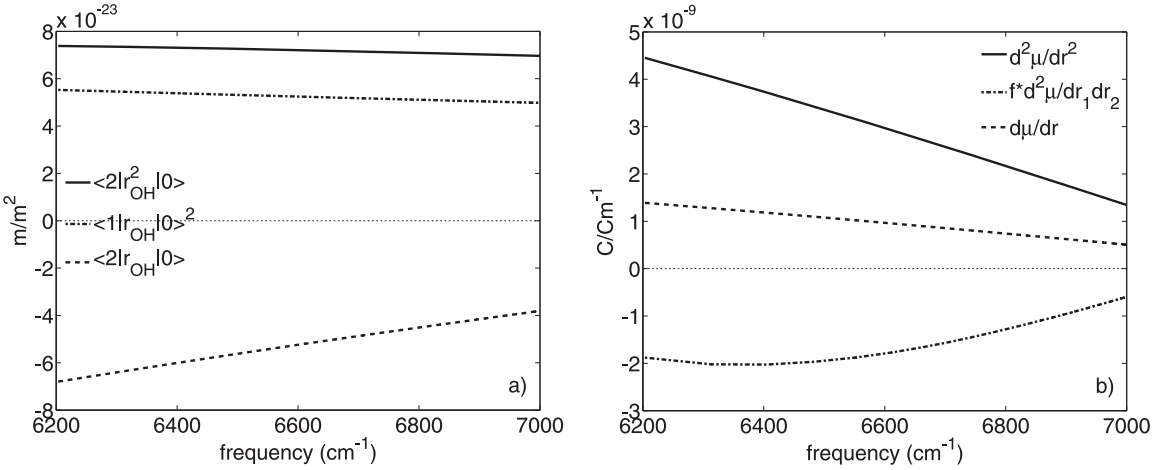

FIG. 5: Left panel: The matrix elements $\langle 2|r_{OH}|0\rangle$, $\langle 2|r_{OH}^2|0\rangle$, and $\langle 1|r_{OH1}|0\rangle\langle 1|r_{OH1}|0\rangle$ as a function of ω_{02}, calculated with the LS model described in the text. The matrix element $\langle 2|r_{OH}|0\rangle$ is divided by 10^{10} for comparison; Right panel: The dipole derivatives $d\hat{\mu}/dr_{OH}$, $d^2\hat{\mu}/dr_{OH}^2$, and $d^2\hat{\mu}/dr_{OH1}dr_{OH2}$ as a function of $\omega_{\rm ov} = \omega_{02}$, calculated with the LS model described in the text. The values of the derivative $d\hat{\mu}/dr_{OH}$ with unit C are multiplied by 10^{10} to facilitate the comparison with $d^2\hat{\mu}/dr_{OH}^2$, and $d^2\hat{\mu}/dr_{OH1}dr_{OH2}$ with unit C/m.

where $\omega_f = 3719.65\,\mathrm{cm}^{-1}$ is the absorption frequency of the free OH-stretch mode in the gas phase. The second derivative of the dipole moment $d^2\hat{\mu}/dr_1^2$ has the following empirical dependence on the fundamental transition frequency ω_{01}[18]:

$$\frac{d^2\hat{\mu}}{dr_{OH}^2}(\omega_{01}) \approx \left(-4.233 + \sqrt{49.983 + \frac{32.086\omega_{01}}{\omega_f}}\right) \cdot 10^{-8} Cm^{-1}; \qquad (14)$$

It follows from these expressions that the first and the second derivatives of the dipole moment both increase with decreasing frequency ω_{01} (i.e. decreasing R_{OO}). The LS model provides the relation between ω_{01} and the hydrogen-bond length R_{OO}, and between R_{OO} and the overtone transition frequency ω_{02}. In the following we will assume that $\omega_{\rm ov} = \omega_{02}$, which implies that we assume that the energy of the two-exciton state is the same as that of the constituting $v = 2$ states of the local O–H oscillator. This assumption is valid in case the exciton states are not strongly delocalized[28]. Hence, using the LS model, $d\hat{\mu}/dr_{OH}(\omega_{01})$ of equation (13) and $d^2\hat{\mu}/dr_{OH}^2(\omega_{01})$ of equation (14) can be transferred to $d\hat{\mu}/dr_{OH}(\omega_{\rm ov})$ and $d^2\hat{\mu}/dr_{OH}^2(\omega_{\rm ov})$ for the overtone transition. The two derivatives of the dipole moment are presented in Figure 5b. Both derivatives increase

with decreasing transition frequency $\omega_{\rm ov}$, i.e. with increasing hydrogen-bond strength. This behavior follows from the fact that lengthening of r_{OH} and shortening of the H...O coordinate is accompanied by transfer of electron density to the oxygen atom to which the H atom is bound. This electron transfer becomes more pronounced with decreasing H...O distance, i.e. with increasing hydrogen-bond strength, thus increasing the derivative of the dipole moment with respect to r_{OH}.

The number density $N_{\rm ov}(\omega_{\rm ov})$ can be obtained using the LS model and the fundamental absorption spectrum. For the fundamental absorption spectrum a similar expression applies as equation (11):

$$\sigma_{01}(\omega_{01}) = \frac{\pi\omega_{01}N_{01}(\omega_{01})}{3\hbar c\varepsilon_0}|\mu_{10}(\omega_{01})|^2 \tag{15}$$

The value of $\mu_{10}(\omega_{01})$ can be calculated with equation (5), keeping only the linear term and using equation (13) and the $\langle 1|\, r\, |0\rangle$ matrix elements obtained with the LS model. The thus calculated $\mu_{10}(\omega_{01})$ and the measured fundamental absorption cross-section $\sigma_{01}(\omega_{01})$ can be used to evaluate the number density $N_{01}(\omega_{01})$. The LS model provides the relation between the transition frequencies ω_{01} and ω_{02}, and thus allows the transfer of $N_{01}(\omega_{01})$ to $N_{\rm ov}(\omega_{\rm ov} = \omega_{02})$.

The only unknown parameter in equation (11) for the overtone transition dipole moment is the parameter $f(\omega_{\rm ov})d^2\hat{\mu}/dr_{OH1}dr_{OH2}$. We determine this parameter by fitting equation (11) to the measured overtone spectrum. In Figure 5 the resulting $f(\omega_{\rm ov})d^2\hat{\mu}/(dr_{OH1}dr_{OH2})$ is presented as a function of the two-exciton transition frequency. It is seen that the absolute value of $f(\omega_{\rm ov})d^2\hat{\mu}/dr_{OH1}dr_{OH2}$ decreases with increasing transition frequency, i.e. with decreasing hydrogen-bond strength (higher $\omega_{\rm ov}$). As for the case of $d^2\hat{\mu}/dr_{OH}^2$, this behavior follows from the increase in electron transfer between the oxygen atoms of the hydrogen-bonded water molecules when the O–H$\cdots$O hydrogen bonds become stronger. An interesting observation is that $f(\omega_{\rm ov})d^2\hat{\mu}/dr_{OH1}dr_{OH2}$ has a negative sign. This negative sign can be explained in the following way. Increasing r_{OH1} of one of the O–H groups will increase the negative charge on the oxygen atom of the hydrogen-bond donating molecule, meaning that the other O–H group acquires increasing OH^- character. The increase in OH^- character means that the O–H$\cdots$O hydrogen bond that is donated along the other O–H coordinate, i.e. r_{OH2}, becomes weaker. Weakening of the hydrogen bond along r_{OH2} means that the derivative of the dipole moment with respect to this coordinate decreases. Hence, increasing r_{OH1} will decrease the derivative of the dipole moment with respect to the r_{OH2} coordinate, thus explaining the negative sign of $f(\omega_{\rm ov})d^2\hat{\mu}/dr_{OH1}dr_{OH2}$.

In Figure 6 the overtone spectrum and the different calculated contributions to the transi-

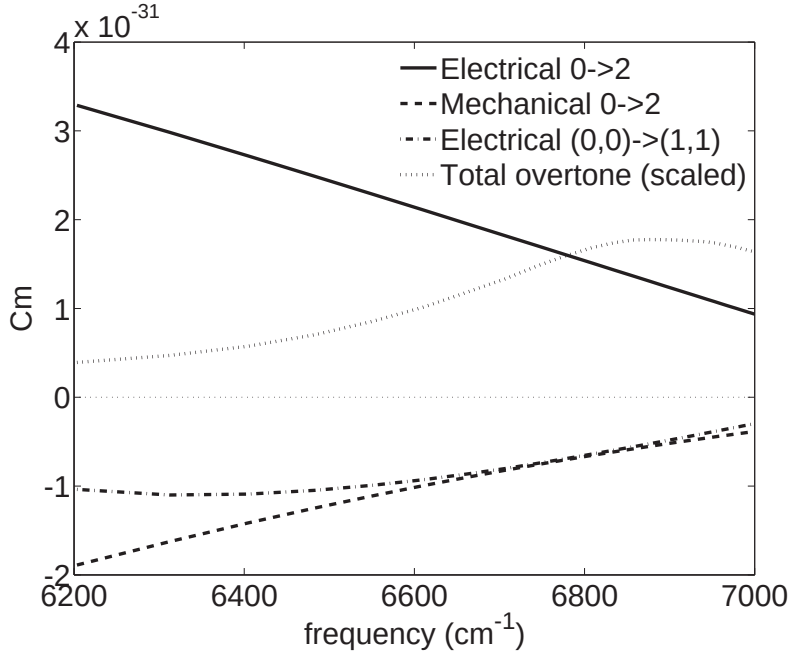

FIG. 6: Contributions to the transition dipole moment $\mu_{\rm ov}$ of the O–H stretch overtone absorption of liquid H_2O. The mechanical anharmonic contribution associated with the excitation of $v = 2$ states (dashed line) and the electrical contribution associated with the excitation of two $v = 1$ states (dashed-dotted line) are opposite in sign to the the electrical contribution associated with the excitation of $v = 2$ states (long dashes). The resulting overtone spectrum is shown as the solid line.

tion dipole moment $\mu_{\rm ov}$ are presented. It is seen that the contribution of the mechanical anharmonicity ($d\hat{\mu}/dr_{OH}\langle 2|r_{OH}|0\rangle(\omega_{\rm ov})$) decreases quite strongly with increasing frequency. This decrease can be understood from the fact that the vibrational potential of the O–H stretch vibration becomes more symmetric with increasing hydrogen-bond length. As the (harmonically forbidden) matrix element $\langle 2|\, r_{OH}\, |0\rangle$ relies on the asymmetry of the vibrational potential, this matrix element strongly decreases. The contributions of the electrical anharmonicities ($\frac{1}{2}d^2\hat{\mu}/dr_{OH}^2\langle 2|r_{OH}^2|0\rangle(\omega_{\rm ov})$ and $f(\omega_{\rm ov})d^2\hat{\mu}/dr_{OH1}dr_{OH2}\langle 1|r_{OH1}|0\rangle\langle 1|r_{OH2}|0\rangle(\omega_{\rm ov})$) decrease less strongly because the value of the quadratic matrix element and the product of the allowed linear matrix elements hardly change with increasing hydrogen-bond strength. The quadratic matrix element hardly changes with increasing hydrogen-bond length because this matrix element is determined by the overall width of the $V_{LS}(r_{OH})$ O–H stretch vibrational potential which is only slightly affected when the R_{OO} hydrogen-bond length changes.

Figure 6 illustrates that there is destructive quantum interference between the positive elec-

trical anharmonic contribution $\frac{1}{2}d^2\hat{\mu}/dr_{OH}^2\langle 2|r_{OH}^2|0\rangle(\omega_{\rm ov})$ associated with the excitation of local $v = 2$ states, and the negative contributions associated with the mechanical anharmonic constribution $d\hat{\mu}/dr_{OH}\langle 2|r_{OH}|0\rangle(\omega_{\rm ov})$ associated with the excitation of local $v = 2$ states and the electrical anharmonic contribution $f(\omega_{\rm ov})d^2\hat{\mu}/dr_{OH1}dr_{OH2}\langle 1|r_{OH1}|0\rangle\langle 1|r_{OH2}|0\rangle(\omega_{\rm ov})$ associated with the excitation of two $v = 1$ states that are located on the same H_2O molecule. This destructive interference is particularly effective at low $\omega_{\rm ov}$ frequencies, thereby strongly reducing the overtone cross-section in this frequency region. At higher frequencies the electrical anharmonic contribution $\frac{1}{2}d^2\hat{\mu}/dr_{OH}^2\langle 2|r_{OH}^2|0\rangle(\omega_{\rm ov})$ dominates over the other contributions, thus providing a significant cross-section to the overtone transition. Hence, the dominance of weakly hydrogen-bonded H_2O molecules in the overtone spectrum is explained from the cancelation of the electrical and mechanical anharmonic contributions to the excitation probability of two-exciton states that involve strongly hydrogen-bonded H_2O molecules.

Discussion

The overtone spectrum of liquid H_2O has a high center frequency and is relatively narrow and smooth. We explain these properties from the destructive quantum interference of the mechanical and electrical anharmonic contributions in the excitation probability of two-exciton states in liquid H_2O. For the isotopically diluted aqueous system of HDO molecules in D_2O, the overtone spectrum of the O–H stretch vibration was found to show distinct structure[18], which means that the shape of this spectrum strongly differs from that of the overtone spectrum of the O–H stretch vibrations of liquid H_2O. The structure of the overtone spectrum of isotopically diluted HDO:D_2O has been explained from a similar quantum interference effect of electrical and mechanical anharmonic contributions to the transition probability[18]. Here we explain the shape and frequency of the overtone spectrum of liquid H_2O from a similar quantum interference effect. However, the overtone absorption of HDO molecules in D_2O only involves the excitation of $v = 2$ states of local O–H stretch vibration of HDO molecules, whereas for H_2O the overtone excitation includes the excitation of delocalized two-exciton states that also include two $v = 1$ excitations located on different O–H groups. This additional contribution makes the O–H overtone spectrum of H_2O essentially different from that of HDO molecules dissolved in D_2O. As the two-exciton states of H_2O are of mixed $v_i = 2$ and $v_i = 1, v_j = 1$ character, the induced absorption band with a central frequency of 2850 cm^{-1} that we observe following the overtone excitation in H_2O (Fig. 2a) will

be a mixture of $v = 2 \rightarrow 3$ and $v = 1 \rightarrow 2$ transitions.

The results of Fig. 5 show that the matrix elements and the dipole derivatives depend on the transition frequency. This so-called non-Condon effect is most pronounced for the contributions to the overtone involving the excitation of local $v = 2$ states. Both the mechanical and the electrical anharmonic interactions associated with this excitation increase significantly with decreasing transition frequency, i.e. with increasing hydrogen-bond strength. A similar non-Condon effect has been observed for the fundamental O–H stretch transitions of liquid water. It was found that the value of μ_{01} strongly increases with increasing strength of the hydrogen bond donated by the O–H group[2]. This non-Condon effect implies that the number density of weakly hydrogen-bonded O–H groups with fundamental transition frequencies $>3500\,\mathrm{cm}^{-1}$ is substantially larger than expected from the spectral intensity of the fundamental O–H stretch absorption spectrum[2,33–35]. For the overtone transition, the non-Condon effects are present in the separate anharmonic contributions to the transition probability, but their influence on the shape of the overtone spectrum is overwhelmed by the effect of the interference of these contributions.

The induced absorption following overtone excitation relaxes with a time constant of 400±50 fs to 540±40 fs (depending on the excitation frequency), which represents a limited range of relatively long relaxation time constants compared to the range of relaxation time constants of 250-550 fs that we recently observed for the one-exciton O–H stretch vibrational state of liquid H_2O[11]. In this latter study it was observed that the time constant increases with the frequency of the fundamental $v = 0 \rightarrow 1$ transition frequency of the O–H stretch vibration, from 250 fs at 3100 cm^{-1} to 550 fs at 3700 cm^{-1}. It thus appears that the relaxation time constants observed for the two-exciton states only match with the high-frequency range of the one-exciton O–H stretch states.

To explain the observation of a limited range of relatively long relaxation time constants of the two-exciton states, it should be realized that the one-exciton states at low O–H stretch frequencies relax exceptionally fast. The time constant of ∼250 fs of this relaxation is for instance much shorter than the vibrational lifetime of 740 fs of the $v = 1$ state of the O–H stretch vibration of isotopically diluted water, i.e. HDO dissolved in D_2O. The short lifetime of the one-exciton states of the O–H stretch vibration of H_2O has been explained from the strong near-resonant coupling of these states to the overtone of the H–O–H bending mode at ∼3300 cm^{-1}.[5,6,10,26,27] For HDO dissolved in D_2O the overtone of the H–O–D bending mode bending mode is at 2900 cm^{-1} and thus far out of resonance with the O–H stretch vibration at ∼3400 cm^{-1}. A similar situation arises for

the two-exciton states of the O–H stretch vibration of H_2O. Due to the destructive quantum interference of the mechanical and electrical anharmonic contributions to the excitation probability, the two-exciton states have relatively high energies around 6900 cm^{-1}. The energy difference with the one-exciton states that are centered around 3300 cm^{-1} is thus $\sim$3600 cm^{-1}. As a result, the energy difference between the two-exciton and the one-exciton states will be in poor resonance with the overtone of the bending mode, thus explaining their relatively slow relaxation. This explanation is supported by the fact that the observed range of relaxation time constants of the two-exciton states matches quite well with the range of relaxation time constants observed in the high-frequency range of the one-exciton states. For both the one-exciton and the two-exciton states the increase of the vibrational lifetime with frequency can be explained from the increase in energy difference between the energy of the quantum of the O–H stretch vibration that has to be released and the energy of the overtone of the bending mode.

Conclusions

We studied the vibrational relaxation of the overtone transition of the O–H stretch vibrations of liquid H_2O using two-color femtosecond pump-probe spectroscopy. We find that excitation of the overtone leads to an induced absorption signal that relaxes with a time constant that increases from 400$\pm$50 femtoseconds to 540$\pm$40 femtoseconds when the overtone excitation frequency is tuned from 6600 to 7200 cm^{-1}.

The overtone transition of liquid H_2O has a relatively smooth and narrow spectrum and is centered at a high frequency of 6900 cm^{-1}, which indicates that the overtone absorption is dominated by H_2O molecules that donate weak O–H$\cdots$O hydrogen bonds to other H_2O molecules. The dominance of weakly hydrogen-bonded H_2O molecules in the overtone absorption can be well explained from the dependence of the excitation probability of the two-exciton states on the hydrogen-bond interaction strength. The excitation probability of the two-exciton states is governed by the quantum interference of different local anharmonic terms of the vibrational potential energy. These terms comprise the mechanical anharmonic contribution (proportional to $d\hat{\mu}/dr_{OH}\langle 2|r_{OH}|0\rangle$) and the electrical anharmonic contribution (proportional to $\frac{1}{2}d^2\hat{\mu}/dr_{OH}^2\langle 2|r_{OH}^2|0\rangle$), both associated with the excitation of local $v = 2$ states, and the electrical anharmonic contribution associated with the excitation of two $v = 1$ states located on the same H_2O molecule (proportional to $d^2\hat{\mu}/dr_{OH1}r_{OH1}\langle 1|r_{OH1}|0\rangle\langle 1|r_{OH2}|0\rangle$). For a broad range

of hydrogen-bond strengths these contributions nearly cancel. Only for weakly hydrogen-bonded water molecules the electrical anharmonicity associated with the excitation of local $v = 2$ states is significantly stronger than the sum of the mechanical anharmonic contribution and the electrical anharmonic contribution associated with the excitation of two $v = 1$ states located on the same H_2O molecule.

The vibrational relaxation time constants of the two-exciton states (400±50 - 540±40 fs) represents a relatively small range of time constants in comparison to the range of time constants of 250-550 fs that is observed for the relaxation of the one-exciton states of liquid H_2O[11]. The fast relaxation of the one-exciton states in the red wing and the central part of the O–H stretch absorption spectrum of liquid H_2O can be well explained from their near-resonance with the strongly coupled overtone of the H–O–H bending mode[5,6,10,26,27]. The two-exciton vibrational states likely relax down to one-exciton states by transferring part of their energy to the overtone of the bending mode. However, due to the destructive quantum interference effects in the overtone cross-section, the excited two-exciton states have quite high energies, and thus this vibrational relaxation process experiences a substantial energy gap, thereby slowing down the relaxation.

Acknowledgments

This work is part of the research program of the "Stichting voor Fundamenteel Onderzoek der Materie (FOM)", which is financially supported by the "Nederlandse organisatie voor Wetenschappelijk Onderzoek (NWO)".

---

* Electronic address: bakker@amolf.nl

[1] Segtnan, V.; Sasic, S.; Isaksson, T.; Ozaki, Y. Studies on the structure of water using two-dimensional near-infrared correlation spectroscopy and principal component analysis. *Anal. Chem.* **2001**, *73*, 3153-3161.

[2] Schmidt, J. R.; Corcelli, S. A.; Skinner, J. L. Pronounced non-Condon effects in the ultrafast infrared spectroscopy of water. *J. Chem. Phys* **2005**, *123*, 044513.

[3] Woutersen, S.; Bakker H. J. Resonant intermolecular transfer of vibrational energy in liquid water. *Nature* **1999**, *402*, 507-509.

[4] Cowan, M. L.; Bruner, B. D.; Huse, N.; Dwyer, J. R.; Chugh, B.; Nibbering, E. T. J.; Elsaesser, T.; Miller, R. J. D. Ultrafast memory loss and energy redistribution in the hydrogen bond network of liquid H_2O. *Nature* **2005**, *434*, 199-202.

[5] Ashihara, S.; Huse, N.; Espagne, A.; Nibbering, E. T. J.; Elsaesser, T. Vibrational couplings and ultrafast relaxation of the O-H bending mode in liquid H_2O. *Chem. Phys. Lett* **2006**, *424*, 66.

[6] Lindner, J.; Vohringer, P.; Pshenichnikov, M. S.; Cringus, D.; Wiersma, D. A.; Mostovoy, M. Vibrational relaxation of pure liquid water. *Chem. Phys. Lett* **2006**, *421*, 329-333.

[7] Ashihara, S.; Huse, N.; Espagne, A.; Nibbering, E. T. J.; Elsaesser, T. Ultrafast structural dynamics of water induced by dissipation of vibrational energy. *J. Phys. Chem. A* **2007**, *111*, 743.

[8] Lindner, J.; Cringus, D.; Pshenichnikov, M.; Vöhringer, P. Anharmonic bendstretch coupling in neat liquid water. *Chem. Phys.* **2007**, *341*, 326-335.

[9] Kraemer, D.; L.; C. M.; Paarmann, A.; Huse, N.; Nibbering, E. T. J.; Elsaesser, T.; Miller, R. J. D. Temperature dependence of the two-dimensional infrared spectrum of liquid H_2O. *PNAS* **2008**, *105*, 437-442.

[10] Ramasesha, K.; De Marco, L.; Mandal, A.; Tokmakoff, A. Water vibrations have strongly mixed intra- and intermolecular character. *Nature Chem.* **2013**, *5*, 935-940.

[11] van der Post, S.T.; Hsieh, C.-S.; Okuno, M.; Nagata, Y.; Bakker, H.J.; Bonn, M.; Hunger, J. Strong frequency dependence of vibrational relaxation in bulk and surface water reveals sub-picosecond structural heterogeneity. *Nature Comm.* **2015**, *6*, 8384.

[12] Deak, J. C.; Rhea, S. T.; Iwaki, L. K.; Dlott, D. D. Vibrational energy relaxation and spectral diffusion in water and deuterated water. *J. Phys. Chem. A* **2000**, *104*, 4866-4875.

[13] Cringus, D.; Jansen, T. I. C.; Pshenichnikov, M. S.; Wiersma, D. A. Ultrafast anisotropy dynamics of water molecules dissolved in acetonitrile. *J. Chem. Phys* **2007**, *127*, 084507.

[14] Jansen, T.; Cringus, D.; Pshenichnikov, M. Dissimilar dynamics of coupled water vibrations. *J. Phys. Chem. A* **2009**, *113*, 6260-6265.

[15] Sceats, M.; Stavola, M.; Rice, S. A. On the role of Fermi resonance in the spectrum of water in its condensed phases. *J. Chem. Phys* **1979**, *71*, 983.

[16] Nielson, G. Rice, S. A. An improved analysis of the OH stretching spectrum of amorphous solid water. *J. Chem. Phys* **1983**, *78*, 4824.

[17] Sovago, M.; Campen, R.; Wurpel, G.; Müller, M.; Bakker, H.J.; Bonn M. Vibrational response of hydrogen-bonded interfacial water is dominated by intramolecular coupling. *Phys. Rev. Lett.* **2008**, *100*,

173901.

[18] Sceats, M.; Belsley, K. A conjecture on the overtone OH stretching spectrum of HDO in liquid water. *Mol. Phys.* **1980**, *40*, 1389-1400.

[19] Buijs, K.; Chopin G.R. Near-infrared studies of the structure of water. I. Pure water. *J. Chem. Phys.* **1963**, *39*, 2035.

[20] Buijs, K.; Chopin G.R. Assignment of the near-Infrared bands of water and ionic solutions. *J. Chem. Phys.* **1964**, *40*, 3120.

[21] Worley, J.; Klotz, I. Near-infrared spectra of H_2O-D_2O solutions. *J. Chem. Phys* **1966**, *45*, 2868-2871.

[22] Belsley, K.; Sceats, M. The overtone OH stretching Raman spectrum of liquid water. *Chem. Phys. Lett* **1980**, *70*, 504.

[23] Walrafen, G.; Pugh, E. Raman Combinations and stretching overtones from water, heavy water, and NaCl in water at shifts to ca. 7000 cm^{-1}. *J. Solution Chem.* **2004**, *33*, 81-97.

[24] Tauber, M. J.; Mathies, R. A.; Chen, X.; Bradforth, S. E. Flowing liquid sample jet for resonance Raman and ultrafast optical spectroscopy. *Rev. Sci. Instr.* **2003**, *74*, 4958.

[25] Rezus, Y.L.A.; Bakker, H.J. On the orientational relaxation of HDO in liquid water. *J. Chem. Phys.* **2005**, *123*, 114502, 1-7.

[26] Lock, A. J.; Woutersen, S.; Bakker, H. J. Ultrafast energy equilibration in hydrogen-bonded liquids. *J. Phys. Chem. A* **2001**, *105*, 1238-1243.

[27] Lock, A. J. Bakker, H. J. Temperature dependence of vibrational relaxation in liquid H_2O. *J. Chem. Phys* **2002**, *117*, 1708-1713.

[28] Edler, J.; Hamm, P. Self-trapping of the amide I band in a peptide model crystal. *J. Chem. Phys.* **2002**, *117*, 2415.

[29] Lippincott, E.; Schroeder, R. One-Dimensional model of the hydrogen bond. *J. Chem. Phys* **1955**, *23*, 1099-1106.

[30] Rey, R.; Moller, K.B.; Hynes, J.T. Hydrogen-bond dynamics in water and ultrafast infrared spectroscopy. *J. Phys. Chem. A* **2002**, *106*, 11993-11996.

[31] Lawrence, C.P.; Skinner, J.L.. Vibrational spectroscopy of HOD in liquid D_2O III. Spectral diffusion, and hydrogen-bonding and rotational dynamics. *J. Chem. Phys.* **2003**, *118*, 264-272.

[32] Moller, K.B.; Rey, R.; Hynes, J.T. Hydrogen-bond dynamics in water and ultrafast infrared spectroscopy: A theoretical study. *J. Phys. Chem. A* **2004**, *108*, 1275-1289.

[33] Loparo, J. J.; Roberts, S. T.; Tokmakoff, A. Multidimensional infrared spectroscopy of water. II.

Hydrogen-bond switching dynamics. *J. Chem. Phys* **2006**, *125*, 194522.

[34] Auer, B.; Kumar, R.; Schmidt, J. R.; Skinner, J. L. Hydrogen bonding and Raman, IR, and 2D-IR spectroscopy of dilute HOD in liquid D_2O. *PNAS* **2007**, *104*, 14215-14220.

[35] Bakker, H. J.; Skinner, J. L. Vibrational spectroscopy as a probe of structure and dynamics in liquid water. *Chem. Rev.* **2010**, *110*, 1498-1514.